

## A novel radiopharmaceutical for detection of malignant melanoma, based on melanin formation: 3-iodo-4-hydroxyphenyl-L-cysteine

R. NISHII,<sup>1,\*</sup> K. KAWAI,<sup>2</sup> L. GARCIA FLORES II,<sup>2</sup> H. KATAOKA,<sup>3</sup> S. JINNOUCHI,<sup>1</sup> S. NAGAMACHI,<sup>1</sup> Y. ARANO<sup>4</sup> and S. TAMURA<sup>1</sup>

<sup>1</sup>Department of Radiology, <sup>2</sup>Central Research Laboratories, and <sup>3</sup>Department of 2nd Pathology, Miyazaki Medical College, 5200 Kihara, Kiyotake-cho, Miyazaki-gun, Miyazaki 889-1692, Japan; and <sup>4</sup>Faculty of Pharmaceutical Sciences, Chiba University, Yayoi-cho, Chiba 263-8522, Japan

Received 2 May 2002, in revised form 7 October 2002 and accepted 21 October 2002

### Summary

The aim of this study was to develop a new artificial amino acid radiopharmaceutical labelled with radioiodine for detection of malignant melanoma, based on melanin formation. By considering the affinity for tyrosinase, a starting enzyme on the branching point to melanin biosynthesis, 3-[<sup>125</sup>I]iodo-4-hydroxyphenyl-L-cysteine (<sup>125</sup>I-L-PC) was synthesized and evaluated biologically. Labelling of <sup>125</sup>I-L-PC using the chloramine-T method was carried out conveniently and efficiently in a short period of time, with high specific activity. In a biodistribution study, <sup>125</sup>I-L-PC showed a low accumulation in normal tissue and relative retention in B16 melanoma. A high contrast image of peripheral tumour was obtained during autoradiography. During an *in vitro* accumulation study, inhibition of <sup>125</sup>I-L-PC with a tyrosinase inhibitor suggested interaction of this tracer with tyrosinase. It indicates that the uptake mechanism of <sup>125</sup>I-L-PC to melanoma tissue was dependent on high tyrosinase activity in melanoma cells. Thus, <sup>125</sup>I-L-PC appears to be a promising radioiodinated amino acid radiopharmaceutical for imaging malignant melanoma in relation to melanin formation, namely specific metabolism with high tyrosinase activity. (© 2003 Lippincott Williams & Wilkins)

**Keywords:** 3-[<sup>125</sup>I]iodo-4-hydroxyphenyl-L-cysteine, malignant melanoma, tyrosinase, amino acid radiopharmaceutical.

### Introduction

Melanin biosynthesis of melanocytes is an essential metabolic pathway for melanomas. It consists of conversion of tyrosine to dopa and then to dopaquinone by tyrosinase oxidation (Fig. 1). In malignant melanoma, melanin formation is associated with high tyrosinase activity and has been the target of antimelanoma chemotherapeutic agents [1]. Graham *et al.* [2] and Wick [3] reported a possible mechanism of selective toxicity of catechols to melanoma cells. A similar attempt to use a

melanin precursor as an antitumour agent has also been reported [4].

As antimelanoma chemotherapeutic agents that are sulfur homologues of tyrosinase substrates, 4-hydroxyphenyl-L-cysteine, 4-hydroxyphenyl-L-cysteamine, and its *N*-acetyl and *N*-propionyl derivatives were synthesized by Ito *et al.* [5] and Miura *et al.* [6]. These compounds have also been reported to have selective cytotoxicity to human neoplastic cells, especially to tyrosinase positive melanoma cells. However, there is no irreversible damage to amelanotic, tyrosinase negative cells [5–7].

In recent years, the contribution of nuclear medicine to oncology has expanded, particularly in the field of tumour imaging. Where radiological techniques aim at anatomical delineation of tumour, nuclear medicine specializes on its physiology. Thereby the focus of interest is shifting from tumour detection to tumour

\*Address all correspondence to Dr Ryuichi Nishii, Department of Radiology, Miyazaki Medical College, 5200 Kihara, Kiyotake-cho, Miyazaki-gun, Miyazaki 889-1692, Japan.  
e-mail: rnishii@post1.miyazaki-med.ac.jp

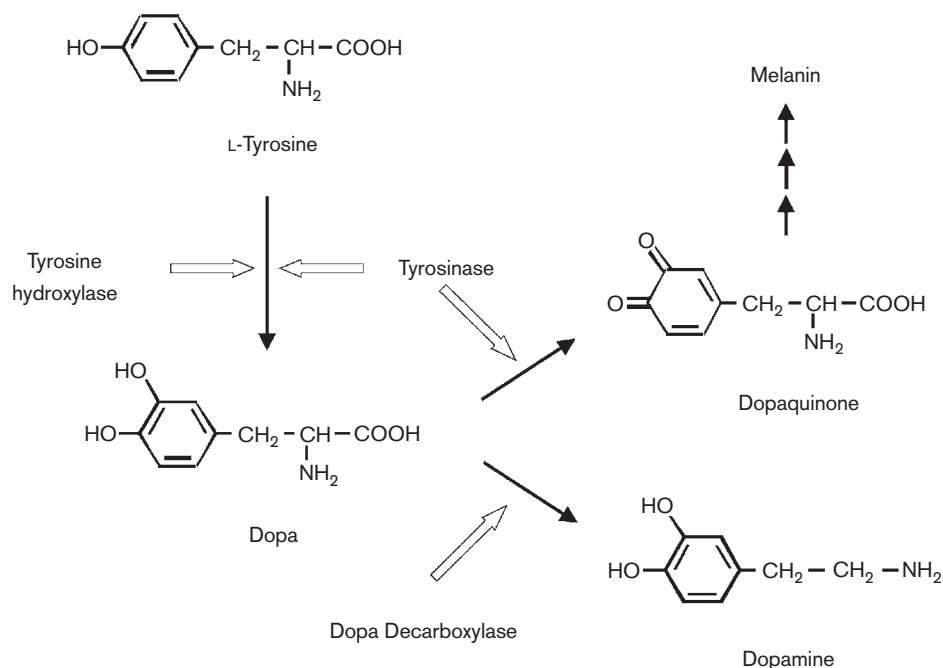


Fig. 1. Metabolic pathway of melanin formation.

characterization [8]. A number of radiopharmaceuticals with affinity to melanin have been synthesized, but few have achieved clinical application for early detection of metastasis, staging, follow-up and radionuclide therapy of melanoma [8].

The authors have developed and investigated radioiodinated tyrosine derivatives such as 3-[ $^{123}\text{I}$ ]iodo- $\alpha$ -methyl-L-tyrosine ( $^{123}\text{I}$ -L-AMT) [9, 10]. It has been proven to be a metabolically stable radiopharmaceutical and has high tissue affinity to the amino acid active transport.  $^{123}\text{I}$ -L-AMT also has been introduced for imaging tumours [11]. It has been reported to be taken up in brain tumour, reflecting amino acid transport and is suitable for single photon emission computed tomography (SPECT) studies [12].

For melanoma specific detection based on its melanin biosynthesis, development of a new radiopharmaceutical that could interact with elevated tyrosinase activity is essential. 4-Hydroxyphenyl-L-cysteine (4-L-PC), a tyrosine derivative with a phenol moiety that provides a site for easy iodination, was selected as a tyrosinase substrate analogue. Introduction of iodine and sulfur to the L-tyrosine molecule would give metabolic stability and rapid renal excretion [9, 13]. This would lead to low background and high contrast in tumour imaging. 3-Iodo-4-hydroxyphenyl-L-cysteine (Fig. 2), a new artificial amino acid radiopharmaceutical labelled with radioiodine, which can be widely available for SPECT studies, was prepared and evaluated.

## Materials and methods

### Synthesis of 4-hydroxyphenyl-L-cysteine

4-hydroxyphenyl-L-cysteine (4-L-PC) was synthesized according to the modified method described by Miura *et al.* [6]. All chemicals used were of reagent grade. A mixture of 28.2 g (300 mmol) of phenol and 18.0 g (75 mmol) of L-cystine was added in 500 ml of 47% HBr and refluxed for 2 h (Fig. 2). The solution was evaporated with 15 ml of thioglycolic acid. The residue was dissolved in water and was adjusted to approximately pH 5 with sodium acetate. After a week of refrigeration, colourless plates were obtained. Isomeric purity was confirmed by high-performance liquid chromatography (HPLC) using the modified method of Somayaji *et al.* [14] which was performed on a Nova Pak  $\text{C}_{18}$  (Waters) column. The 4-L-PC was separated from the 2-hydroxy isomer using water as the eluent.

The structure of 4-L-PC was confirmed by  $^1\text{H}$  NMR, mass spectrometry and elemental analysis. For  $^1\text{H}$  NMR:  $\delta$  3.33 (2H, d,  $J=5.5$  Hz,  $\text{CH}_2$ ), 4.28 (1H, t,  $J=5.5$  Hz, CH), 6.95 (2H, d,  $J=8.5$  Hz, Ar-H2 and H6), 7.47 (2H, d,  $J=8.5$  Hz, Ar-H3 and H5). For mass spectrometry: MH (+) 214. For elemental analysis, calculated for  $\text{C}_9\text{H}_{11}\text{NO}_3\text{S}$ : H 5.20%, C 50.69%, N 6.57%, O 22.52%, S 15.01%. Found: H 5.09%, C 49.53%, N 6.36%.

It was clear that only the L-configuration of the amino acid was obtained, since a single peak was found with the

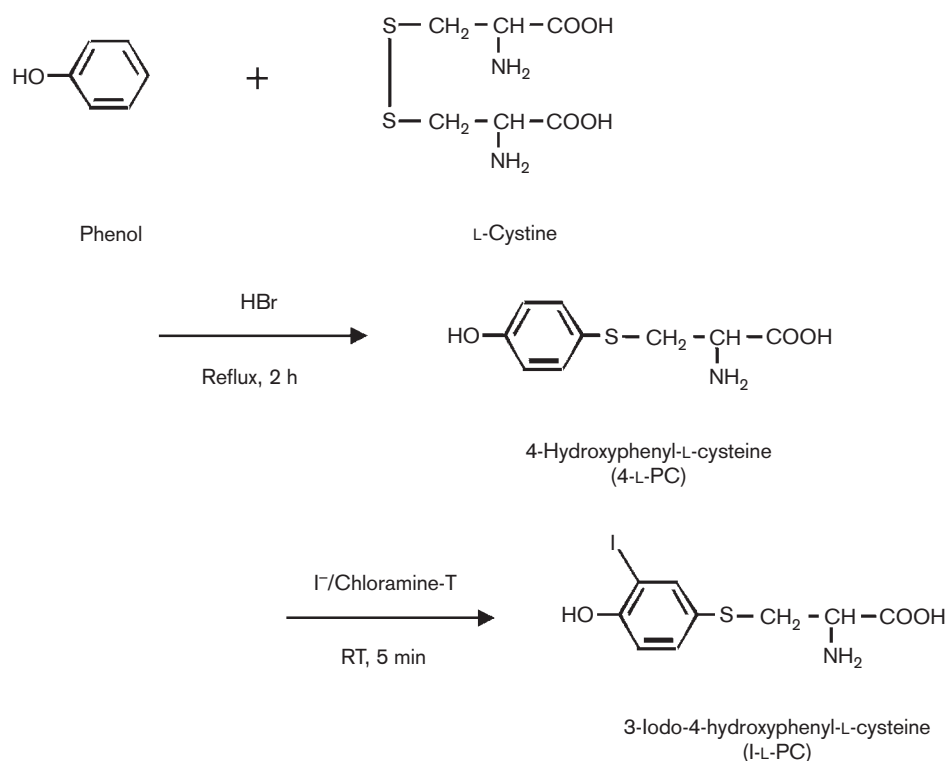


Fig. 2. Chemical reaction and radioiodination of 3-iodo-4-hydroxyphenyl-L-cysteine. RT, room temperature.

chiral HPLC, performed on Crownpak CR (–) (Daicel) column. The retention time of 4-L-PC at a flow rate of  $0.5 \text{ ml}\cdot\text{min}^{-1}$  was 16 min.

#### Preparation of 3-[ $^{125}\text{I}$ ]iodo-4-hydroxyphenyl-L-cysteine

$^{125}\text{I}$ -L-PC was prepared by the chloramine-T method under a no-carrier added condition [9] (Fig. 2). Chloramine-T (Aldrich) at a concentration of  $1.0 \times 10^{-8} \text{ mol}$  in  $10 \mu\text{l}$  of  $0.05 \text{ M}$  phosphate buffer (pH 8.5) was added to a mixture of 4-L-PC ( $1.0 \times 10^{-7} \text{ mol}$ ) in  $10 \mu\text{l}$  of phosphoric acid and no-carrier added  $\text{Na}^{125}\text{I}$  (Amersham) in  $80 \mu\text{l}$  of  $0.4 \text{ M}$  phosphate buffer (pH 8.5). Five minutes later,  $1.0 \times 10^{-8} \text{ mol}$  of sodium metabisulfite in  $10 \mu\text{l}$  of  $0.05 \text{ M}$  phosphate buffer (pH 8.5) was added to stop the reaction.

$^{125}\text{I}$ -L-PC was purified by HPLC, performed on Nova Pak  $\text{C}_{18}$  (Waters) column using 15% v/v acetic acid as eluent at a flow rate of  $0.5 \text{ ml}\cdot\text{min}^{-1}$  (retention times:  $^{125}\text{I}$ -L-PC, 38 min;  $^{125}\text{I}$ , 6 min; unlabelled 4-L-PC, 28 min).

The labelling efficiency and radiochemical purity were examined by thin-layer chromatography using silica gel (Merck; Art. 5553) and three solvent systems: methanol/acetic acid, 100:1 ( $R_F$  values:  $^{125}\text{I}$ -L-PC, 0.45–0.55;  $^{125}\text{I}$ , 0.70–0.80); methanol/10% ammonium acetate, 10:1 ( $R_F$  values:  $^{125}\text{I}$ -L-PC, 0.50–0.60;  $^{125}\text{I}$ , 0.75–0.85); and ethanol/

ammonia solution (28%), (Nacalai Tesque), 3:1 ( $R_F$  values:  $^{125}\text{I}$ -L-PC, 0.40–0.50;  $^{125}\text{I}$ , 0.65–0.75).

#### Tumour cells

B16 melanoma cells obtained from the Riken Cell Bank were cultured in Dulbecco's Modified Eagle's Medium (DMEM) (Sigma) medium containing 10% of fetal bovine serum (Gibco). B16 melanoma was maintained in our laboratory by serial transplantation in C57BL6 mice for 2 week intervals. The tumour was dissociated in saline solution. Then the suspension was centrifuged at  $500 \times g$  for 10 min, and the sediment was suspended in saline. Melanoma cells ( $1 \times 10^6$ ) in  $0.3 \text{ ml}$  saline were injected subcutaneously on the right thigh of a 6-week-old C57BL6 male mouse. Ten days later, the tumour became palpable and was examined. The experimental procedures were in accordance with the guidelines on the use of living animals for scientific investigation which were established in our institution.

#### Biodistribution in normal mice

Biodistribution of  $^{125}\text{I}$ -L-PC was determined using ddY male mice (6 weeks old) as amelanotic ones.  $^{125}\text{I}$ -L-PC

(37 kBq) in 100  $\mu$ l of saline was injected via the tail vein. The mice were killed by ether anaesthesia at various time intervals, and the organs of interest were rapidly dissected. The radioactivity in weighed tissue samples was measured using a gamma counter (Aloka; ARC-1000M). Data are expressed in mean  $\pm$  SD per cent injected dose per g wet tissue.

#### *Biodistribution in B16 melanoma-bearing mice*

Biodistribution of  $^{125}\text{I}$ -L-PC in B16 melanoma-bearing C57BL6 mice was performed using the same method mentioned above. Moreover, 3- $^{125}\text{I}$ iodo- $\alpha$ -methyl-L-tyrosine ( $^{125}\text{I}$ -L-AMT) was compared with  $^{125}\text{I}$ -L-PC at 15 min intervals.  $^{125}\text{I}$ -L-AMT was prepared from  $\alpha$ -methyl-L-tyrosine (Aldrich) using our previously described method [9]. The radioactivity in tissue samples was measured using a gamma counter (Aloka; ARC-360).

#### *Autoradiography*

A tumour-bearing C57BL6 mouse was injected with 100  $\mu$ l of  $^{125}\text{I}$ -L-PC (1.85 MBq) intravenously and was killed by ether anaesthesia 60 min after the tracer injection. For whole body autoradiography, the mouse was frozen in an embedding medium at  $-15^\circ\text{C}$  for 24 h and then was sliced using an Autocryotome (Nakagawa; NA-200F). After drying overnight, freeze-dried slices were placed in contact with the imaging plate (Fuji Photo Film; BAS-TR2040) for 10 days. Images were processed with a Bio-Imaging Analyzer (Fuji Photo Film; BAS-2000).

#### *In vitro accumulation study in B16 melanoma cells*

Melanoma cells ( $5 \times 10^5$ ) in 0.9 ml of HEPES buffer (pH 7.4) were preincubated for 10 min for temperature equilibration. The 0.1 ml of the buffer containing radioactive tracers was added and incubated at  $37^\circ\text{C}$  for 30 min. Inhibition studies of the membrane active transport and tyrosinase, the starting enzyme of melanin formation, were carried out using  $5 \times 10^{-4}$  M ouabain (Sigma),  $1 \times 10^{-3}$  M L-tyrosine (Sigma) and  $1 \times 10^{-4}$  M phenylthiourea (PTU) (Aldrich), respectively, added before preincubation.

At the end of incubation period, the cells were trapped on a glass filter (Advantec; GC-50) and were washed twice with the ice-cold buffer under air vacuum. The radioactivities of the cells were measured and the accumulation percentage of the injected dose per each sample was then calculated.

To further investigate the localization in melanosome, a cell fraction study was performed. After the incubation, each sample was centrifuged at 800 rpm ( $130 \times g$ ) for

5 min. The supernatant was removed and the tumour cells were suspended in 0.25 M sucrose. The suspension of melanoma cells was homogenized using a Potter-Elvehjem homogenizer (Iuchi) and was centrifuged according to the method of Menon and Haberman [15] using ultracentrifugation (Tomy, SRX-200). The radioactivity of the precipitate was measured as the melanin granule fraction.

#### *Measurement of partition coefficients*

The partition coefficients of  $^{125}\text{I}$ -L-PC was measured using 2.0 ml of *n*-octanol as the organic phase and 2.0 ml of 0.1 M phosphate buffer (pH 7.0 for tumour tissue and pH 7.4 for plasma) as the aqueous phase. The *n*-octanol and the buffer were pre-mixed twice using a mechanical mixer for 1 min at room temperature. Then, 20  $\mu$ l of  $^{125}\text{I}$ -L-PC in saline was added and mixed twice for 1 min at room temperature. The radioactivity of 200  $\mu$ l of each phase was measured after centrifugation [13].

## **Results**

#### *Radiosynthesis*

Chemical reaction and iodination of 3-iodo-4-hydroxyphenyl-L-cysteine are shown in Fig. 2. A labelling efficiency of more than 65% resulted in the labelling of 4-L-PC to  $^{125}\text{I}$ -L-PC. After the purification, no-carrier added  $^{125}\text{I}$ -L-PC with a radiochemical purity greater than 95% was obtained and separation from unlabelled 4-L-PC, which had biological activity, was confirmed.

#### *Biodistribution in normal mice*

Table 1 summarizes the distribution data of  $^{125}\text{I}$ -L-PC in normal mice. Blood clearance was faster than other metabolically stable radioiodinated amino acids such as  $^{125}\text{I}$ -L-AMT [10]. The accumulation of  $^{125}\text{I}$ -L-PC in the kidney and the liver reached the highest value within 3 min post-injection of tracer and the radioactivity rapidly decreased without re-uptake of this tracer. Meanwhile, less accumulation was observed in the pancreas and brain, which have been known for their high utilization of amino acids. Furthermore, the accumulation in the stomach was not elevated, indicating metabolic stability against de-iodination in the *in vivo* study.

#### *Biodistribution in B16 melanoma-bearing mice*

The biodistribution study of  $^{125}\text{I}$ -L-PC in the B16 melanoma is shown in Table 2. The tumour accumula-

tions at 5 min and 60 min were  $1.71 \pm 0.27\%$  and  $0.35 \pm 0.21\%$  injected dose per g (ID/g) tissue. Higher accumulation was observed in the tumour than in the skin and muscle at 60 min. Rapid blood clearance was

also noted. The comparison of the tumour-to-blood ratio and the tumour-to-muscle ratio between  $^{125}\text{I-L-PC}$  and  $^{125}\text{I-L-AMT}$  is summarized in Table 3. The tumour-to-blood ratio of  $^{125}\text{I-L-PC}$  reached approximately 1 at

**Table 1.** Biodistribution of  $^{125}\text{I-L-PC}$  in normal ddY mice.

Organ	Time (min)							
	1	2	3	5	10	15	30	60
Blood	$6.23 \pm 0.67$	$4.31 \pm 0.49$	$3.29 \pm 0.95$	$2.58 \pm 0.08$	$1.52 \pm 0.12$	$0.99 \pm 0.13$	$0.41 \pm 0.09$	$0.14 \pm 0.04$
Brain	$0.30 \pm 0.05$	$0.18 \pm 0.02$	$0.26 \pm 0.27$	$0.16 \pm 0.09$	$0.07 \pm 0.01$	$0.04 \pm 0.01$	$0.01 \pm 0.09$	<0.01
Pancreas	$3.35 \pm 0.63$	$1.93 \pm 0.33$	$1.27 \pm 0.40$	$0.99 \pm 0.07$	$0.71 \pm 0.25$	$0.47 \pm 0.10$	$0.16 \pm 0.03$	$0.07 \pm 0.02$
Spleen	$1.55 \pm 0.16$	$1.46 \pm 0.39$	$1.08 \pm 0.66$	$0.79 \pm 0.16$	$0.36 \pm 0.02$	$0.24 \pm 0.03$	$0.07 \pm 0.04$	$0.02 \pm 0.01$
Stomach	$0.96 \pm 0.14$	$0.62 \pm 0.11$	$0.95 \pm 0.43$	$0.77 \pm 0.15$	$1.95 \pm 0.71$	$2.41 \pm 0.71$	$0.62 \pm 0.11$	$1.23 \pm 0.45$
Intestine	$1.10 \pm 0.20$	$0.89 \pm 0.13$	$0.83 \pm 0.21$	$1.03 \pm 0.36$	$1.95 \pm 1.18$	$2.24 \pm 1.76$	$1.41 \pm 0.20$	$2.52 \pm 1.64$
Adrenal gland	$1.19 \pm 0.40$	$1.22 \pm 0.18$	$0.74 \pm 0.56$	$2.95 \pm 4.34$	$0.48 \pm 0.19$	<0.01	<0.01	<0.01
Kidney	$18.71 \pm 5.51$	$30.04 \pm 3.14$	$31.46 \pm 9.68$	$24.12 \pm 3.04$	$15.79 \pm 2.39$	$9.05 \pm 1.62$	$5.87 \pm 4.91$	$1.93 \pm 2.11$
Liver	$4.73 \pm 0.60$	$4.79 \pm 0.30$	$3.63 \pm 1.07$	$3.79 \pm 1.41$	$2.64 \pm 0.56$	$1.39 \pm 0.62$	$0.46 \pm 0.13$	$0.33 \pm 0.12$
Heart	$4.01 \pm 0.82$	$2.35 \pm 0.33$	$1.47 \pm 0.38$	$1.16 \pm 0.11$	$0.60 \pm 0.05$	$0.38 \pm 0.06$	$0.35 \pm 0.30$	$0.02 \pm 0.01$
Lung	$4.04 \pm 0.70$	$3.05 \pm 0.31$	$2.31 \pm 0.55$	$2.00 \pm 0.25$	$1.29 \pm 0.14$	$0.94 \pm 0.15$	$0.41 \pm 0.04$	$0.15 \pm 0.03$
Eyeball	$0.75 \pm 0.27$	$0.85 \pm 0.60$	$0.77 \pm 0.64$	$0.74 \pm 0.63$	$0.26 \pm 0.09$	$0.14 \pm 0.09$	<0.01	<0.01

%ID/g tissue, mean  $\pm$  (SD) for 3–4 mice.

**Table 2.** Biodistribution of  $^{125}\text{I-L-PC}$  in B16 melanoma-bearing C57BL6 mice.

Organ or tumour	Time (min)				
	5	15	30	60	120
Blood	$4.82 \pm 0.44$	$2.07 \pm 0.07$	$0.56 \pm 0.12$	$0.41 \pm 0.04$	$0.30 \pm 0.07$
Brain	$0.18 \pm 0.01$	$0.07 \pm 0.01$	$0.02 \pm 0.01$	$0.01 \pm 0.00$	$0.01 \pm 0.00$
Pancreas	$1.92 \pm 0.21$	$0.84 \pm 0.03$	$0.24 \pm 0.05$	$0.41 \pm 0.24$	$0.07 \pm 0.02$
Spleen	$1.12 \pm 0.03$	$0.52 \pm 0.08$	$0.18 \pm 0.03$	$0.01 \pm 0.02$	$0.13 \pm 0.03$
Stomach	$1.36 \pm 0.33$	$0.02 \pm 0.38$	$3.59 \pm 2.88$	$5.55 \pm 4.25$	$1.53 \pm 0.17$
Intestine	$2.70 \pm 0.11$	$2.28 \pm 1.27$	$3.39 \pm 0.25$	$5.79 \pm 2.12$	$3.37 \pm 0.46$
Kidney	$53.87 \pm 6.32$	$20.48 \pm 1.58$	$4.09 \pm 1.98$	$1.50 \pm 0.59$	$0.49 \pm 0.05$
Liver	$5.76 \pm 0.45$	$2.17 \pm 0.20$	$1.02 \pm 0.30$	$1.44 \pm 0.32$	$0.56 \pm 0.16$
Heart	$1.89 \pm 0.26$	$0.71 \pm 0.01$	$0.18 \pm 0.07$	$0.18 \pm 0.07$	$0.07 \pm 0.02$
Lung	$3.18 \pm 0.11$	$1.65 \pm 0.10$	$0.41 \pm 0.05$	$0.32 \pm 0.03$	$0.29 \pm 0.07$
Tumour	$1.71 \pm 0.27$	$0.86 \pm 0.17$	$0.43 \pm 0.03$	$0.35 \pm 0.21$	$0.12 \pm 0.04$
Muscle	$1.01 \pm 0.01$	$0.26 \pm 0.14$	$0.09 \pm 0.03$	$0.05 \pm 0.03$	$0.02 \pm 0.01$
Skin	$2.72 \pm 0.15$	$1.44 \pm 0.21$	$0.48 \pm 0.17$	$0.24 \pm 0.03$	$0.11 \pm 0.02$
Eyeball	$0.71 \pm 0.16$	$0.32 \pm 0.14$	$0.11 \pm 0.05$	$0.05 \pm 0.01$	$0.04 \pm 0.01$

%ID/g tissue, mean  $\pm$  (SD) for three mice.

**Table 3.** Tumour-to-blood ratios and tumour-to-muscle ratios after intravenous injection of tumour-seeking tracers in B16 melanoma-bearing C57BL6 mice.

Amino acid	Tumour-to-blood ratio			Tumour-to-muscle ratio		
	5 min	15 min	60 min	5 min	15 min	60 min
$^{125}\text{I-L-PC}$	$0.38 \pm 0.07$	$0.50 \pm 0.16$	$0.97 \pm 0.48$	$1.84 \pm 0.03$	$3.55 \pm 0.84$	$6.47 \pm 0.76$
$^{125}\text{I-L-AMT}$	$1.13 \pm 0.11$	$2.22 \pm 0.69$	$1.87 \pm 0.38$	$4.86 \pm 0.57$	$4.26 \pm 0.36$	$3.62 \pm 0.59$

All values were for three mice.

60 min after injection. Tumour-to-muscle ratios increased up to 6.67 at 60 min after  $^{125}\text{I}$ -L-PC injection and were higher than  $^{125}\text{I}$ -L-AMT. The results showed relative retention in melanoma tissue of  $^{125}\text{I}$ -L-PC.

#### Autoradiography

Fig. 3 shows autoradiograms obtained at 60 min after intravenous injection of  $^{125}\text{I}$ -L-PC to a melanoma-bearing mouse. The tumour image was clearly visualized with high contrast to soft tissue. Low accumulation in the brain and the lung supported the results of the biodistribution study. No uptake into areas of necrosis was noted on this image. The specific localization within the tumour itself is of particular interest for clinical imaging.

#### In vitro accumulation study in B16 melanoma cells

The accumulation of  $^{125}\text{I}$ -L-PC ( $3.03 \pm 0.10\%$  ID per  $5 \times 10^5$  melanoma cells) was similar to  $^{125}\text{I}$ -L-AMT. Table 4 shows the percentage effect of control accumulation with inhibitor loading. Significant inhibition of  $^{125}\text{I}$ -L-AMT was noted with ouabain ( $P < 0.05$ ) and L-tyrosine

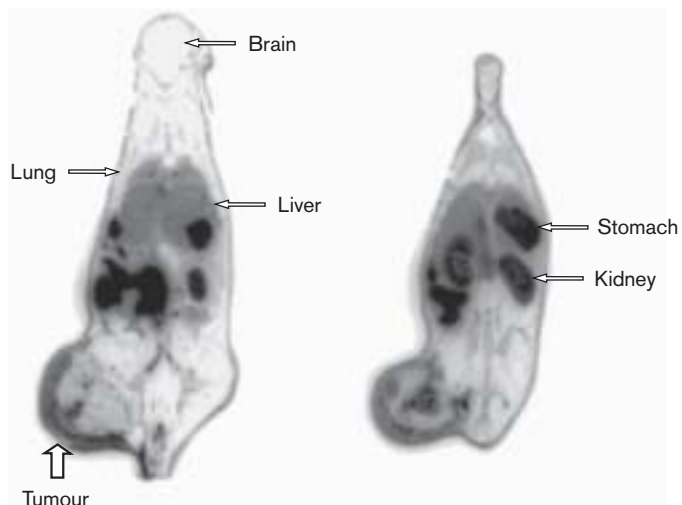


Fig. 3. Autoradiography of a mouse bearing B16 melanoma injected with  $^{125}\text{I}$ -L-PC.

Table 4. Effects of inhibition on tracer accumulation in B16 melanoma cells.

Amino acid	Ouabain	L-Tyrosine	Phenylthiourea
$^{125}\text{I}$ -L-PC	$113.66 \pm 15.82$	$77.59 \pm 14.94$	$55.24 \pm 12.32^*$
$^{125}\text{I}$ -L-AMT	$72.64 \pm 0.87^*$	$58.32 \pm 2.48^*$	$84.82 \pm 5.37$

Per cent of control accumulation, mean  $\pm$  (SD); \* $P < 0.05$ .

( $P < 0.05$ ), while there was no significant inhibition in  $^{125}\text{I}$ -L-PC. With PTU, a specific tyrosinase inhibitor, a stronger inhibitory effect on the accumulation of  $^{125}\text{I}$ -L-PC ( $P < 0.05$ ) was noted in contrast to  $^{125}\text{I}$ -L-AMT.

In a cell fraction study, high localization of  $^{125}\text{I}$ -L-PC (37.3% of the total cell uptake) in melanin granule fraction was observed different from  $^{125}\text{I}$ -L-AMT (4%). The radioactivity of  $^{125}\text{I}$ -L-PC, especially in the melanosome fraction, was also reduced after pretreatment with PTU.

#### Partition coefficients

The role of partition coefficients in  $^{125}\text{I}$ -L-PC was also evaluated (Table 5). The partition coefficients of  $^{123}\text{I}$ -L-AMT and  $^{14}\text{C}$ -L-tyrosine are also shown as references, which were previously reported [9, 13]. The lipophilicity of  $^{125}\text{I}$ -L-PC was higher than that of  $^{123}\text{I}$ -L-AMT and  $^{14}\text{C}$ -L-tyrosine.

#### Discussion

In malignant melanoma, the synthesis of melanin is highly elevated because of a marked increase of tyrosinase activity [16]. Many attempts have been made to develop rational chemotherapy for this disease by taking advantage of this unique physiological process of melanin synthesis. Ito and Miura have synthesized various phenolic compounds as substrates for tyrosinase [5, 6], and they found that 4-L-PC was a good substrate of mammalian tyrosinase for forming melanin-like pigments [17].

Affinity to melanoma tissue, with elevated tyrosinase activity, is of paramount importance in detecting melanoma. In the present study, which aimed to develop a new radiopharmaceutical for detecting malignant melanoma based on its melanin biosynthesis, 4-L-PC was selected as a mother compound for iodination. It is a tyrosine derivative of tyrosinase substrates with a phenol moiety which provides a site for easy iodination. In addition, radioiodination and sulfurization of the tyrosine molecule were expected to result in metabolic stability and rapid excretion [9, 13].

Table 5. Partition coefficients of  $^{125}\text{I}$ -L-PC,  $^{123}\text{I}$ -L-AMT and  $^{14}\text{C}$ -tyrosine at pH 7.0 and 7.4.

Amino acid	pH 7.0	pH 7.4
$^{125}\text{I}$ -L-PC	$-0.28 \pm 0.04$	$-0.37 \pm 0.04$
$^{123}\text{I}$ -L-AMT	$-0.88 \pm 0.00$	$-0.91 \pm 0.00$
$^{14}\text{C}$ -tyrosine	$-1.98 \pm 0.02$	$-2.00 \pm 0.05$

log (*n*-octanol/0.1 M phosphate buffer).

An amino acid in the L-configuration is required for affinity of biological mechanism. After one step of chemical reaction and separation of the 2-hydroxy isomer, only the L-configuration of 4-PC was obtained. The labelling efficiency of  $^{125}\text{I}$ -L-PC was from 65% to 82%, and the radiochemical purity was greater than 95%. It was shown that our labelling procedure conveniently gave high labelling efficiency and high specific activity in a short time. Because radioiodine has the advantage of availability, low cost, adequate half-life and radiation energy, radiopharmaceuticals labelled with radioiodine are widely used for SPECT imaging. Use of  $^{131}\text{I}$  could be available for radiotherapy.

In the biodistribution study of  $^{125}\text{I}$ -L-PC in normal ddY mice, blood clearance and renal excretion were faster than those of metabolically stable radioiodinated amino acids such as  $^{125}\text{I}$ -L-AMT [10]. Meanwhile, less accumulation was observed in pancreas and brain in which  $^{125}\text{I}$ -L-AMT showed high accumulation (Table 1). Because of non-affinity to normal organs,  $^{125}\text{I}$ -L-PC showed unique characteristics as an L-amino acid. The rapid clearance of this tracer from normal organs and relative retention in the tumour was also noted in the biodistribution study in B16 melanoma-bearing mice (Table 2). When compared with  $^{125}\text{I}$ -L-AMT, which are available for clinical use, tumour-to-muscle ratios increased up to 6.67 at 60 min after  $^{125}\text{I}$ -L-PC injection and were higher than  $^{125}\text{I}$ -L-AMT.

In order to visualize malignant melanoma and metastases, a potential radiopharmaceutical must meet important criteria: high tumour-to-tissue (blood, muscle, brain, liver or lung) ratios. In spite of non-affinity of  $^{125}\text{I}$ -L-PC to normal tissue, tumour-to-blood ratio reached approximately 1 at 60 min after injection. Tumour-to-muscle ratio increased up to 6.67 at 60 min after injection of this tracer (Table 3). This result indicates relative retention of the tracer in the melanoma. Therefore,  $^{125}\text{I}$ -L-PC has the potential of good contrast in a tumour-seeking agent.

Indeed, autoradiography in B16 melanoma-bearing mouse showed tumour localization of radioactivity after injection of  $^{125}\text{I}$ -L-PC (Fig. 3). It provided a clear delineation of the tumour. We noted that, on autoradiographic images, there was less uptake into the necrotic region. The specific localization within the tumour itself is of particular interest for clinical imaging. It is considered that  $^{125}\text{I}$ -L-PC could be a suitable radiopharmaceutical for imaging melanoma.

Furthermore, the accumulation of  $^{125}\text{I}$ -L-PC in melanotic tissues, the skin and the uvea, in C57BL6 mouse was higher than that in amelanotic ddY mouse. This suggested that the localization of  $^{125}\text{I}$ -L-PC could be related to the biosynthesis of melanin.

In *in vitro* accumulation study with B16 melanoma cells, ouabain which is an efficient  $\text{Na}^+$ - $\text{K}^+$  ATPase

inhibitor has been used to suppress the  $\text{Na}^+$  dependent concentrative uptake of amino acids [18]. L-tyrosine has been used as a competitive inhibitor of the neutral amino acid transport [9, 19]. No inhibitory effect of ouabain and L-tyrosine on the uptake of  $^{125}\text{I}$ -L-PC suggested less involvement of amino acid active transport for  $^{125}\text{I}$ -L-PC accumulation into the melanoma cells. This lower participation of amino acid transport accounts for the lower accumulation in the brain and the pancreas in contrast with high cerebral and pancreatic accumulation of  $^{125}\text{I}$ -L-AMT, a marker of amino acid transport.

Although the transport system of  $^{125}\text{I}$ -L-PC is less related by amino acid active transport, it is considered that the relative increase of lipophilicity of this tracer could explain the permeability into cells.

In inhibition studies, PTU is frequently used as a tyrosinase inhibitor in melanin biosynthesis [20]. PTU had an inhibitory effect on only the accumulation of  $^{125}\text{I}$ -L-PC (Table 4). The decrease in the uptake of  $^{125}\text{I}$ -L-PC with PTU indicated that  $^{125}\text{I}$ -L-PC interacted with tyrosinase and that is similar to 4-L-PC. Furthermore, the specific localization of  $^{125}\text{I}$ -L-PC in melanin granule fractions supports these results. In melanoma cells, it interacts with tyrosinase confirmed by PTU inhibition and then localized in melanin granules fraction. The interaction with tyrosinase and the localization in melanin granules might lead to the retention of this compound in melanoma cells.

In summary, the preparation of  $^{125}\text{I}$ -L-PC was carried out conveniently and efficiently in a short period of time, with high specific activity. The biodistribution of  $^{125}\text{I}$ -L-PC showed low accumulation in normal tissue and relative retention in B16 melanoma. The high imaging contrast of peripheral tumour obtained with this tracer is ideal for clinical application. *In vitro* accumulation study revealed an interaction of  $^{125}\text{I}$ -L-PC with tyrosinase. It indicates that the accumulation and retention of  $^{125}\text{I}$ -L-PC to melanoma tissue is dependent on high tyrosinase activity in melanoma. With affinity to tyrosinase activity,  $^{125}\text{I}$ -L-PC could image melanoma tissue with specificity and might be able to determine the viability of tumour cells. Moreover, because I-L-PC accumulated low in normal tissue, it might be applied as a therapeutic radiopharmaceutical when labelled with  $^{131}\text{I}$ .

## Conclusion

I-L-PC, a new artificial amino acid radiopharmaceutical, has a high potential for diagnosis and treatment of malignant melanoma. Its accumulation in melanoma was dependent on high tyrosinase activity in melanin formation.

## References

1. Jimbow K, Miura T, Ito S, Ishikawa K. Phenolic melanin precursors provide a rational approach to design of antitumor agents for melanoma. *Pig Cell Res* 1989; **2**: 34–39.
2. Graham GD, Tiffany SM, Vogel FS. The toxicity of melanin precursors. *J Invest Dermatol* 1978; **70**: 113–116.
3. Wick MM. Levodopa and dopamine analogs as DNA polymerase inhibitors and antitumor agents in human melanoma. *Cancer Res* 1980; **40**: 1414–1418.
4. Yamada K, Jimbow K, Engelhardt R, Ito S. Selective cytotoxicity of phenolic melanin precursor, 4-S-cysteaminylphenol, on *in vitro* melanoma cell. *Biochem Pharmacol* 1989; **38**: 2217–2221.
5. Ito S, Inoue S, Yamamoto Y, Fujita K. Synthesis and antitumor activity of cysteinyl-3,4-dihydroxyphenylalanines and related compounds. *J Med Chem* 1981; **24**: 673–677.
6. Miura S, Ueda T, Jimbow K, Ito S, Fujita K. Synthesis of cysteinylphenol, cysteaminyphenol, and related compounds, and *in vivo* evaluation of antimelanoma effect. *Arch Dermatol Res* 1987; **279**: 219–225.
7. Ito S, Kato T, Ishikawa K, Kasuga T, Jimbow K. Mechanism of selective toxicity of 4-S-cysteinylphenol and 4-S-cysteaminyphenol to melanocytes. *Biochem Pharmacol* 1987; **36**: 2007–2011.
8. Hoefnagel CA. Role of nuclear medicine in melanoma. *Eur J Nucl Med* 1998; **25**: 1567–1574.
9. Kawai K, Fujibayashi Y, Saji H, et al. A strategy for the study of cerebral amino acid transport using iodine-123-labeled amino acid radiopharmaceutical: 3-iodo-alpha-methyl-L-tyrosine. *J Nucl Med* 1991; **32**: 819–824.
10. Kawai K, Fujibayashi Y, Yonekura Y, et al. An artificial amino acid radiopharmaceutical for single photon emission computed tomographic study of pancreatic amino acid transports: <sup>123</sup>I-3-iodo-alpha-methyl-L-tyrosine. *Anal Nucl Med* 1992; **6**: 169–175.
11. Jager PL, Franssen EJJ, Kool W, et al. Feasibility of tumor imaging using L-3-[iodine-123]-iodo- $\alpha$ -methyl-tyrosine in experimental tumors. *J Nucl Med* 1998; **39**: 1736–1743.
12. Langen KJ, Roosen N, Coenen HH. Brain and brain tumor uptake of L-3-[<sup>123</sup>I]iodo-alpha-methyl-tyrosine: competition with natural L-amino acids. *J Nucl Med* 1991; **32**: 1225–1228.
13. Kawai K, Flores II LG, Nakagawa M, et al. Brain uptake of iodinated L-meta-tyrosine, a metabolically stable amino acid derivative. *Nucl Med Commun* 1999; **20**: 153–157.
14. Somayaji V, Ito S, Jimbow K, Wiebe LI. The synthesis of 4-S-cysteinyl-[U-<sup>14</sup>C]phenol, an experimental antimelanoma agent. *Appl Radiat Isot* 1989; **40**: 539–540.
15. Menon IA, Haberman HF. Isolation of melanin granules. *Methods Enzymol* 1974; **31**: 389–394.
16. Pawelek JM. Factors regulating growth and pigmentation of melanoma cells. *J Invest Dermatol* 1976; **66**: 201–209.
17. Jimbow K, Ito S, Maeda K, et al. Mechanism regulating selective growth inhibition disintegration of melanoma cells by 4-S-cysteinyl phenol and related compounds. *J Invest Dermatol* 1985; **84**: 355–360.
18. Hughes CCW, Lantos PL. Uptake of leucine and alanine by cultured cerebral capillary endothelial cells. *Brain Res* 1989; **480**: 126–132.
19. Oxender DL, Christensen HN. Distinct mediating systems for the transport of neutral amino acids by the Ehrlich cell. *J Biol Chem* 1963; **238**: 3686–3699.
20. Prezioso JA, Epperly MN, Wang N, Bloomer WD. Effects of tyrosinase activity on the cytotoxicity of 4-S-cysteaminyphenol and N-acetyl-4-S-cysteaminyphenol in melanoma cells. *Cancer Lett* 1992; **63**: 73–79.